A Letters Journal Exploring the Frontiers of Physics

August 2015

EPL, **111** (2015) 47004
doi: 10.1209/0295-5075/111/47004

www.epljournal.org

Multiferroic property of colloidal crystals with three-dimensional solid-solid phase transitions

J. P. Huang[(a)], X. Y. Shen and Y. X. Chen

Department of Physics, State Key Laboratory of Surface Physics, and Collaborative Innovation Center of Advanced Microstructures, Fudan University - Shanghai 200433, China

received 29 April 2015; accepted in final form 10 August 2015
published online 3 September 2015

PACS 75.85.+t – Magnetoelectric effects, multiferroics
PACS 64.70.kj – Glasses
PACS 47.57.J- – Colloidal systems

Abstract – It is a challenge to understand the dynamics of ubiquitous solid-solid phase transitions in three dimensions. In this direction, colloidal crystals are often adopted as a model system for investigation, because they contain highly ordered arrays of colloidal microparticles, analogous to atomic or molecular counterparts with appropriate scaling. Here, by resorting to the Ewald-Kornfeld formulation, we describe a type of solid-solid phase transitions from the body-centered tetragonal lattice, to the face-centered cubic lattice, and then to subsequent lattices, which have been experimentally demonstrated in electro-magnetorheological fluids (which contain suspended microparticles enabling the formation of crystalline structures) subjected to crossed electric and magnetic fields. As a result, we find that each lattice exhibits specific multiferroic properties at room temperature. The findings are further confirmed by independent finite-element simulations. Despite some limitations (*e.g.*, the specific value of change in magnetization is small during phase transitions), this work suggests a way to real-time measure the microscopic dynamics of three-dimensional solid-solid phase transitions in colloidal crystals by detecting their multiferroic properties.

Introduction. – Solid-solid phase transitions appear to be ubiquitous, say, in metals, alloys and minerals [1]. They are particularly important in many fields like geoscience and the production of diamond or steel. However, the microscopic dynamics of solid-solid phase transitions are still not well understood. In this direction, colloidal crystals are often adopted as a model system for investigation. This is because a colloidal crystal contains highly ordered arrays of colloidal particles, which is analogous to its atomic or molecular counterparts with appropriate scaling. The relevant research is productive: for instance, very recently, Han and coauthors [2] have revealed a two-step nucleation mechanism in solid-solid phase transitions by utilizing a single-particle resolution video microscopy of *two-dimensional* colloidal films of diameter-tunable microspheres. However, the methods for directly detecting *three-dimensional* solid-solid phase transitions are still far from being satisfactory, which prohibit both better control of the underlying dynamics and further development of a relevant theory. Accordingly, here we propose a different method for detecting three-dimensional solid-solid phase transitions in real time.

To proceed, let us first introduce the study of couplings among multiple physical fields, which is always a fundamental challenge in the discipline of physics and has helped to realize a number of new materials with novel functions: say, thermoelectric materials (coupling thermal fields and electric fields) transferring waste heat into electricity [3], photoelectric materials (with a coupling between light fields and electric fields) producing electricity upon the incidence of light [4], piezoelectric materials (bridging pressure fields and electric fields) yielding electricity from pressure [5], and multiferroic materials (coupling magnetic fields and electric fields) enabling to control magnetization (or electric polarization) with an electric (or a magnetic) field [6–11]. Recent years have witnessed significant achievements in the study of such multiferroic materials; these materials are particularly important in technological applications like information storage [12,13] and magnetic-field sensors [14,15].

[(a)] E-mail: jphuang@fudan.edu.cn

Inspired by the above-mentioned achievement by Han and his coauthors who studied the two-dimensional phase transitions in colloidal films [2], here we suggest to utilize the detection of multiferroic properties to measure the three-dimensional solid-solid phase transitions in colloidal crystals. For this purpose, let us first introduce a typical class of electro-magnetorheological (EMR) fluids [16–23]. Generally, electrorheological or magnetorheological fluids, which are composed of ferroelectric or ferromagnetic microparticles like $BaTiO_3$ or Fe_3O_4 in a carrier liquid (say, silicone oil), can be changed from a liquid to a semi-solid (namely, a colloidal crystal or colloidal supracrystal [24]) by acting an external direct-current (DC) electric or magnetic field; the underlying mechanism is due to the formation of columnar crystallites of these microparticles. It is well known that the ground state (which is equivalent to "the steady structure" in this work) of the columnar crystallites in either electrorheological or magnetorheological fluids is body-centered tetragonal (BCT) [25,26]. In fact, EMR fluids have the properties of both electrorheological and magnetorheological fluids since the microparticles suspended in EMR fluids have both magnetic and electric responses. That is, EMR fluids can also be changed into a colloidal crystal (EMR colloidal crystal) by adding either (both) an electric field or (and) a magnetic field. However, since the ground states of electrorheological and magnetorheological fluids are both BCT [25,26], EMR colloidal crystals are known to have different structures when an external DC electric field is perpendicular to an external DC magnetic field [18,19]. Concretely, for EMR colloidal crystals, experimental researches [19] have shown a structural phase transition at room temperature from the BCT lattice to the face-centered cubic (FCC) lattice as the magnetic and electric fields vary accordingly. However, the transition dynamics has not been explicitly formulated in theory until this work. In particular, let us take the electric-field (E_0) direction as the x-direction and the magnetic-field (H_0) direction as the z-direction. Reference [19] has experimentally shown that for a large E_0 ($E_0 \neq 0$) and a zero H_0 ($H_0 = 0$), the ground state of the EMR colloidal crystal is BCT; as H_0 becomes large enough, say $H_0 = H_{FCC}(\gg 0)$, the state changes into a FCC lattice [19]. Clearly, when H_0 lies between 0 and H_{FCC}, the state corresponds to intermediate lattices between BCT and FCC lattices. This process allows us to study magnetic-field control of electric polarization in EMR colloidal crystals. Owing to the magnetic and electric symmetry existing in EMR colloidal crystals, a similar scenario holds as well. Namely, for $H_0 \neq 0$ and $E_0 = 0$, the ground state of EMR colloidal crystals is BCT; as E_0 is large enough, say $E_0 = E_{FCC}(\gg 0)$, the state corresponds to a FCC lattice. Evidently, when E_0 lies between 0 and E_{FCC}, the state is characterized by intermediate lattices between BCT and FCC lattices. The scenario allows us to investigate electric-field control of magnetization in EMR colloidal crystals. In what follows, we shall only focus on the electric-field control of magnetization because it is more applicable than magnetic-field control of electric polarization due to the fact that electric fields can be generated more easily than magnetic fields in experiments; certainly the same formalism works also for the magnetic-field control of electric polarization in EMR colloidal crystals as long as one replaces magnetic permeabilities with electric permittivities appropriately. And similar results could be obtained.

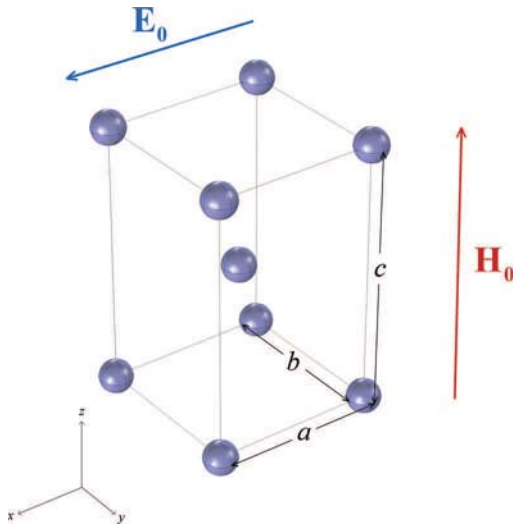

Fig. 1: (Color online) Schematic graph showing the location of two spherical microparticles in a tetragonal unit cell with one fourfold rotational axis along the z-direction; one microparticle is located at the center and the other one at a corner; for clarity, the microparticles are not shown to the scale. The three lattice constants are a, b, and c along the x-, y-, and z-direction, respectively; we have $a = b$ due to symmetry. The electric (or magnetic) field, E_0 (or H_0), is along the x (or z) direction.

Theory. – Now we are in a position to explicitly formulate the above-mentioned room temperature structural phase transition of EMR colloidal crystals (which are composed of identical, isotropic, spherical microparticles with electric permittivity ϵ_1 and magnetic permeability μ_1 in a homogeneous carrier liquid with ϵ_2 and μ_2). Let us start from their ground state for $H_0 \neq 0$ and $E_0 = 0$, the BCT lattice (fig. 1). This BCT lattice can be seen as a tetragonal lattice (fig. 1), plus a basis of two microparticles each of which is fixed with a point dipole at its center. One of the two microparticles is located at the body center of the tetragonal unit cell and the other one at a corner. Its lattice constants are denoted by $a(= b) = \ell q^{-1/2}$ and $c = q\ell$ along the $x\,(y)$ and z axes, respectively. In this case, the uniaxial anisotropic axis is directed along the z-axis. As q varies, the volume of the unit cell keeps the same, $V_c = \ell^3$. Thus, the degree of anisotropy of the tetragonal lattice is measured by how q is deviated from unity. In particular, $q = 0.87358$ and $2^{1/3}$ denotes the BCT and FCC lattice, respectively.

When we apply an x-directed external electric field E_0, the dipole moment in a microparticle, $\vec{p} = p\hat{x}$, are

perpendicular to the uniaxial anisotropic axis along the z-direction. Then, the local field $\vec{E}$ (*i.e.*, $\vec{E} = E_x\hat{x}$) at the lattice point $\vec{R} = \vec{0}$ is given by the Ewald-Kornfeld formulation [27–29],

$$E_x = p\sum_{j=1}^{2}\sum_{\vec{R}\neq\vec{0}}\left[-\gamma_1(R_j) + x_j^2q^2\gamma_2(R_j)\right] - \frac{4\pi p}{V_c}\sum_{\vec{G}\neq\vec{0}}\mho(\vec{G})\frac{G_x^2}{G^2}\exp\left(\frac{-G^2}{4\psi^2}\right) + \frac{4p\psi^3}{3\sqrt{\pi}}. \quad (1)$$

In this equation, the two coefficients γ_1 and γ_2 are given by

$$\gamma_1(r) = \frac{\mathrm{erfc}(\psi r)}{r^3} + \frac{2\psi}{\sqrt{\pi}r^2}\exp(-\psi^2r^2),$$
$$\gamma_2(r) = \frac{3\mathrm{erfc}(\psi r)}{r^5} + \left(\frac{4\psi^3}{\sqrt{\pi}r^2} + \frac{6\psi}{\sqrt{\pi}r^4}\right)\exp(-\psi^2r^2),$$

where $\mathrm{erfc}(\psi r)$ denotes the complementary error function, and ψ an adjustable parameter making the summation converge rapidly, $1 < \psi < 10^{0.6}$. In eq. (1), R and G denote the lattice vector and the reciprocal lattice vector,

$$\vec{R} = \ell(q^{-1/2}l\hat{x} + q^{-1/2}m\hat{y} + qn\hat{z}),$$
$$\vec{G} = \frac{2\pi}{\ell}(q^{1/2}u\hat{x} + q^{1/2}v\hat{y} + q^{-1}w\hat{z}),$$

where l, m, n, u, v, and w are integers. In addition, x_j and R_j in eq. (1) are given by

$$x_j = l - \frac{j-1}{2} \text{ and } R_j = \left|\vec{R} - \frac{j-1}{2}(a\hat{x} + b\hat{y} + c\hat{z})\right|.$$

Also, the structure factor $\mho(\vec{G}) = 1 + \exp[i(u+v+w)/\pi]$.

Now we define a local-field factor in the x-direction, $\beta_x = 3V_cE_x/(4\pi p)$. It is worth noting that β_x is a function of a single variable q. Similarly, we obtain the local-field factors in the y- and z-direction, β_y and β_z. There is a sum rule $\beta_x + \beta_y + \beta_z = 3$ [29,30]. Because the uniaxial anisotropic axis under consideration is along the z-direction, there must be $\beta_x = \beta_y$. For convenience, we set $\beta_x(= \beta_y) \equiv \beta_\perp$ and $\beta_z \equiv \beta_\parallel$. So, there exists $2\beta_\perp + \beta_\parallel = 3$. Next, for obtaining the effective magnetic permeability in the z-direction, $\mu_e^\parallel$, we resort to the anisotropic Maxwell-Garnett formula [31] for magnetism with a high degree of accuracy due to the explicit determination of $\beta_\parallel$ [32],

$$\frac{\mu_e^\parallel - \mu_2}{\beta_\parallel\mu_e^\parallel + (3-\beta_\parallel)\mu_2} = \rho\frac{\mu_1 - \mu_2}{\mu_1 + 2\mu_2}, \quad (2)$$

where ρ is the volume fraction of microparticles in the system. The substitution of $\beta_\parallel = 1$ into eq. (2) yields the well-known (isotropic) Maxwell-Garnett formula for magnetism, whose electric counterpart works well for dielectrics [33–35].

On the other hand, according to the definition of magnetization in electrodynamics [36], we obtain the z-directed magnetization $M_\parallel$ as

$$M_\parallel = \left[\frac{\mu_e^\parallel}{\mu_0} - 1\right]H_0, \quad (3)$$

where μ_0 denotes the magnetic permeability of vacuum. As mentioned above, when $E_0 = 0$, the system has a BCT structure in columnar crystallites, which corresponds to $q = 0.87358$; when E_0 increases up to $E_0 = E_{FCC}$, this system then has a FCC structure instead, which accords with $q = 2^{1/3}$. Without loss of generality, we might as well use the increasing values of q to qualitatively characterize the increasing trend of E_0 from 0 ($q = 0.87358$ of the BCT lattice), to E_{FCC} ($q = 2^{1/3}$ of the FCC lattice), and even to a larger value (say, $q = 1.5$ of a subsequent lattice) in spite of the lack of an explicit expression between q and E_0. Clearly, eq. (3) implies that the magnetization $M_\parallel$ along the z-direction is determined by the electric field E_0 along the x-direction since the $\mu_e^\parallel$ in eq. (3) depends on $\beta_\parallel$ (which is a function of a single variable q) according to eq. (2). In other words, eq. (3) enables us to investigate the electric-field control of magnetization in the EMR system under consideration.

For real applications, we calculate a model EMR colloidal crystal, which is composed of identical, isotropic, spherical Fe_3O_4 microparticles with magnetic permeability μ_c, each having an isotropic $BaTiO_3$ shell with μ_s embedded in silicone oil with μ_2. The volume fraction of the Fe_3O_4 microparticle (core) in each Fe_3O_4-$BaTiO_3$ composite microparticle is f_c. So far, the equivalent magnetic permeability, μ_1, of an individual Fe_3O_4-$BaTiO_3$ composite microparticle can be obtained by solving Laplace's equation of magnetostatics together with appropriate boundary conditions. After some straightforward derivations, we obtain the expression as

$$\mu_1 = \mu_s\frac{\mu_c(1+2f_c) + 2\mu_s(1-f_c)}{\mu_c(1-f_c) + \mu_s(2+f_c)}, \quad (4)$$

which has the same mathematical form as the expression for an electric permittivity [32]. This equation is exact for an isolated Fe_3O_4-$BaTiO_3$ composite microparticle, and it serves as a result of the first-order approximation for such a composite microparticle in the present EMR system by neglecting multipolar effects due to all the other composite microparticles.

Calculations based on the anisotropic Maxwell-Garnett formula. – For calculations, we choose to use the following parameters at room temperature: $\mu_c = 85\mu_0$, $\mu_s = \mu_0$, and $\mu_2 = \mu_0$. Numerical results are shown in fig. 2. According to this figure, it is evident that increasing q (namely, increasing E_0) causes $M_\parallel/H_0$ to decrease; the effect becomes significant, especially for large values of ρ and f_c. Figure 2 clearly shows that an external electric

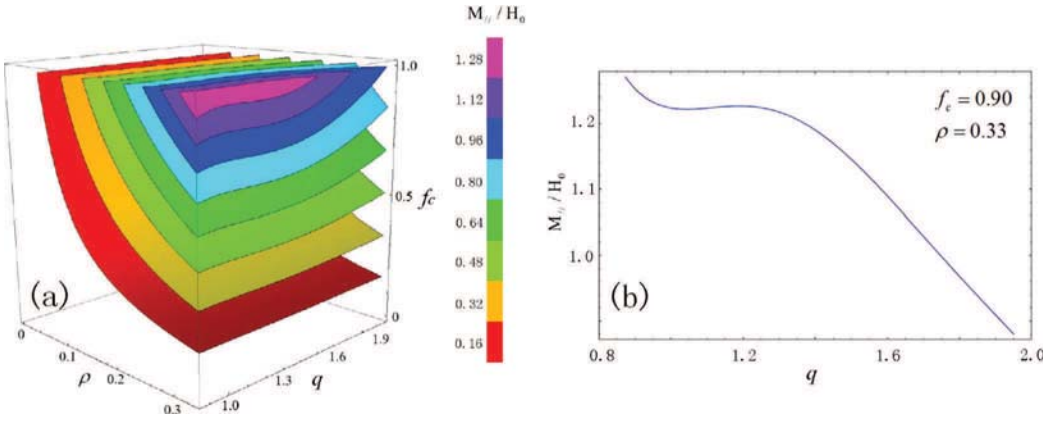

Fig. 2: (Color online) (a) $M_{\|}/H_0$ calculated according to eq. (3) as a function of q, ρ and f_c; (b) $M_{\|}/H_0$ *vs.* q when $f_c = 0.9$ and $\rho = 0.33$: particularly, for the BCT (or FCC) structure, $M_{\|}/H_0 = 1.27$ (or 1.22). Parameters: $\mu_c = 85\mu_0$, $\mu_s = \mu_0$, and $\mu_2 = \mu_0$.

field (E_0) can be used to tune the overall magnetization of the system indeed.

For plotting fig. 2, we have adopted the anisotropic Maxwell-Garnett formula (eq. (2)) to calculate the effective magnetic permeability of the EMR system containing columnar crystallites. The experimental results [19] demonstrated that there exists a structural phase transition from the BCT lattice to the FCC lattice in such columnar crystallites when applying crossed electric and magnetic fields appropriately. The transition process has been taken into account in the above theoretical analysis accordingly. As a result of solid-solid phase transitions, the electric-field control of magnetization has been clearly shown in fig. 2. In other words, each lattice of the EMR colloidal crystal exhibits specific multiferroic properties at room temperature. In order to show the validity of our analysis (fig. 2) based on the anisotropic Maxwell-Garnett formula (eq. (2)), we attempt to investigate further in the following by using a different approach —three-dimensional finite-element simulations.

Three-dimensional finite-element simulations. – Here we utilize the COMSOL Multiphysics software (`http://www.comsol.com/`) to perform three-dimensional finite-element simulations (where the multipolar effects are considered) of electric-field control of magnetization in EMR colloidal crystals; these simulations are essentially free from eqs. (1), (2) and (4), see fig. 3(a)–(i) that shows the simulation results of $M_{\|}/H_0$ for nine spherical Fe_3O_4-$BaTiO_3$ composite microparticles arranged in the lattice structure of the tetragonal unit cell as shown in fig. 1. As a matter of fact, the present arrangement of the nine microparticles accords with a simplified three-dimensional system where one microparticle is located at the center of the four two-microparticle chains directed along the x-axis. According to this figure, one can clearly observe that as the electric field (E_0) increases, namely, q increases, $M_{\|}/H_0$ can be changed accordingly.

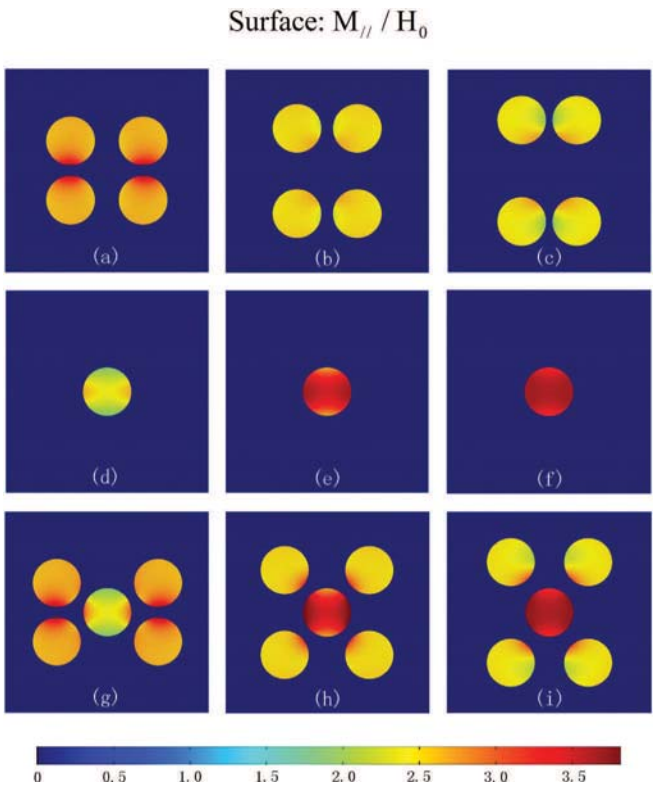

Fig. 3: (Color online) Three-dimensional finite-element simulation results of $M_{\|}/H_0$ represented by color surface. Here we investigate nine spherical Fe_3O_4-$BaTiO_3$ composite microparticles with a diameter of 36 μm, which are arranged in the lattice structure of the tetragonal unit cell shown in fig. 1. Panels (a)–(c) display the (010) plane containing four composite microparticles; panels (d)–(f) show the plane that is parallel to the (010) plane, which contains the composite microparticle located at the body center; panels (g)–(i) depict the (110) plane involving five composite microparticles. (a), (d), (g): $q = 0.87358$ (the BCT lattice); (b), (e), (h): $q = 2^{1/3}$ (the FCC lattice); and (c), (f), (i): $q = 1.5$ (a subsequent lattice). Other parameters: $f_c = 0.95$, $\ell = 50\,\mu$m, $\mu_c = 85\mu_0$, $\mu_s = \mu_0$, and $\mu_2 = \mu_0$.

In detail, let us look at fig. 3(d)–(f). As q increases from (fig. 3(d)) $q = 0.87358$ (the BCT lattice; $E_0 = 0$), to (fig. 3(e)) $q = 2^{1/3}$ (the FCC lattice; $E_0 = E_{FCC}$), and to (fig. 3(f)) $q = 1.5$ (a subsequent lattice; $E_0 > E_{FCC}$), the magnetization $M_{\|}/H_0$ within the composite microparticle located at the body center increases accordingly. On the other hand, we notice that the magnetization $M_{\|}/H_0$ within the other eight composite microparticles generally decreases as q increases; see fig. 3(a)–(c), (g)–(i). As a result, the overall magnetization (which can be explicitly obtained by averaging $M_{\|}/H_0$ over the volume of the whole simulation box) due to the total nine composite microparticles decreases as q increases (or E_0 increases). This echoes with fig. 2 that shows an overall decreasing trend of magnetization of the whole system (which was seen as an effective medium) as q increases (or E_0 increases), especially for larger values of ρ and f_c.

Incidentally, fig. 3 also helps to indicate that one might tailor the microstructure of the EMR colloidal crystal for uses with quite different purposes, say, using an increasing electric field either to reduce magnetization (say, in fig. 3(a)–(c)) or to enhance magnetization (*e.g.*, in fig. 3(d)–(f)).

Discussion and conclusions. – A feature of this work is that we have developed the Ewald-Kornfeld formulation to explicitly describe the experimental scenario reported in ref. [19]. As a result of the effective medium theory (eq. (2)), we found that different lattices of the colloidal crystal exhibit different multiferroic responses at room temperature (fig. 2), which is further confirmed by three-dimensional finite-element simulations (fig. 3).

In ref. [19], the authors used the magnetic free energy density calculated through the Bergman-Milton representation to describe the transition process. The parameters adopted are based on their experiments. Nevertheless, their characterizing parameter is unable to show how the external electric field dynamically controls the magnetization of the whole EMR system satisfactorily. In contrast, here we have given a theoretical model to describe the interplay between the electric field and magnetization.

The focus of this work is on colloidal crystals that contain microparticles located in stable lattices in case of fixed electric and magnetic fields. In fact, if suspended particles are at nanoscale, it is difficult to obtain stable lattices since the influence of Brownian motion becomes more evident. But, in principle, for such cases of nanoparticles, similar multiferroic properties can also come to appear.

In principle, the actual values of E_{FCC} and H_{FCC} depend on the system details, say, volume fractions, material properties, and so on. Thus, for the sake of generality, we have adopted an equivalent parameter of q. In particular, for the reference of future experimental demonstrations, here we would like to mention the specific system reported in ref. [19]: the authors experimentally achieved an FCC lattice at $E_{FCC} = 2\,\mathrm{kV/mm}$ and $H_{FCC} = 54\,\mathrm{G}$.

By using a VSM (vibrating sample magnetometer), one can measure the magnetization process of the whole system, thus yielding the overall magnetization of the system. On the other hand, if one wants to detect the magnetic moment of individual microparticles, he/she may resort to SQUID (superconducting quantum interference detector).

In spite of some limitations (*e.g.*, the specific value of change in magnetization, while undergoing phase transitions, is small), this work proposes a method for a real-time measurement of microscopic dynamics of three-dimensional solid-solid phase transitions in colloidal crystals by detecting multiferroic responses.

* * *

We thank Prof. Y. Z. Wu and Prof. H. J. Xiang for fruitful discussion. We acknowledge the financial support by the NNSFC under Grant No. 11222544, by the Fok Ying Tung Education Foundation under Grant No. 131008, and by the CNKBRSF under Grant No. 2011CB922004.

REFERENCES

[1] Porter D. A., Easterling K. E. and Sherif M. Y., *Phase Transformations in Metals and Alloys* (CRC Press) 2008.
[2] Peng Y., Wang F., Wang Z. R., Alsayed A. M., Zhang Z. X., Yodh A. G. and Han Y. L., *Nat. Mater.*, **14** (2015) 101.
[3] Xu Y., Gan Z. X. and Zhang S. C., *Phys. Rev. Lett.*, **112** (2014) 226801.
[4] Tashenov S. *et al.*, *Phys. Rev. Lett.*, **113** (2014) 113001.
[5] Wu W. Z. *et al.*, *Nature*, **514** (2014) 470.
[6] Kubacka T. *et al.*, *Science*, **343** (2014) 1333.
[7] Artyukhin S., Delaney K. T., Spaldin N. A. and Mostovoy M., *Nat. Mater.*, **13** (2014) 42.
[8] Windsor Y. W. *et al.*, *Phys. Rev. Lett.*, **113** (2014) 167202.
[9] Dong S., Liu J. M. and Dagotto E., *Phys. Rev. Lett.*, **113** (2014) 187204.
[10] Roy K., *EPL*, **108** (2014) 67002.
[11] Murthy J. K., Chandrasekhar K. D., Wu H. C., Yang H. D., Lin J. Y. and Venimadhav A., *EPL*, **108** (2014) 27013.
[12] Roy K., *SPIN*, **3** (2013) 1330003.
[13] Roy K., *Appl. Phys. Lett.*, **103** (2013) 173110.
[14] Wang Y., Li J. and Viehland D., *Mater. Today*, **17** (2014) 269.
[15] Lenz J. and Edelstein A. S., *IEEE Sens. J.*, **6** (2006) 631.
[16] Minagawa K., Watanabe T., Munakata M. and Koyama K., *J. Non-Newtonian Fluid Mech.*, **52** (1994) 59.
[17] Koyama K., Minagawa K., Watanabe T., Kumakura Y. and Takimoto J., *J. Non-Newtonian Fluid Mech.*, **58** (1995) 195.
[18] Tao R. and Jiang Q., *Phys. Rev. E*, **57** (1998) 5761.
[19] Sheng P., Wen W. J., Wang N., Ma H. R., Lin Z. F., Tam W. Y. and Chan C. T., *Physica B*, **279** (2000) 168.

[20] Shibayama A., Miyazaki T., Yamaguchi K., Murakami K. and Fujita T., *Int. J. Mod. Phys. B*, **16** (2002) 2405.
[21] Lu J. B., Yan Q. S., Tian H. and Gao W. Q., *Adv. Mater. Res.*, **135** (2010) 24.
[22] Zhang W. L. and Choi H. J., *Soft Matter*, **10** (2014) 6601.
[23] Zhang W. L. and Choi H. J., *Polymers*, **6** (2014) 2803.
[24] Pileni M. P., *EPL*, **109** (2015) 58001.
[25] Tao R. and Sun J. M., *Phys. Rev. Lett.*, **67** (1991) 398.
[26] Zhou L., Wen W. J. and Sheng P., *Phys. Rev. Lett.*, **81** (1998) 1509.
[27] Ewald P. P., *Ann. Phys. (Leipzig)*, **64** (1921) 253.
[28] Kornfeld H., *Z. Phys.*, **22** (1924) 27.
[29] Lo C. K. and Yu K. W., *Phys. Rev. E*, **64** (2001) 031501.
[30] Landau L. D., Lifshitz E. M. and Pitaevskii L. P., *Electrodynamics of Continuous Media*, 2nd edition (Pergamon Press, New York, U.S.) 1984.
[31] Huang J. P., Wan J. T. K., Lo C. K. and Yu K. W., *Phys. Rev. E*, **64** (2001) 061505.
[32] Gao Y., Huang J. P., Liu Y. M., Gao L., Yu K. W. and Zhang X., *Phys. Rev. Lett.*, **104** (2010) 034501.
[33] Huang J. P. and Yu K. W., *Phys. Rep.*, **431** (2006) 87.
[34] Maxwell-Garnett J. C., *Philos. Trans. R. Soc. London, Ser. A*, **203** (1904) 385.
[35] Maxwell-Garnett J. C., *Philos. Trans. R. Soc. London, Ser. A*, **203** (1906) 237.
[36] Jackson J. D., *Classical Electrodynamics*, 3rd edition (John Wiley & Sons, Inc., U.S.) 1999.